ACS OMEGA

http://pubs.acs.org/journal/acsodf

Article

Modification at the C2′-O-Position with 2-Methylbenzothiophene Induces Unique Structural Changes and Thermal Transitions on Duplexes of RNA and DNA

Cheyenne N. Phillips, Madeline Choi, Kim Ngan Huynh, Haobin Wang,* and Marino J. E. Resendiz*

Cite This: *ACS Omega* 2022, 7, 37782–37796

Read Online

ACCESS | Metrics & More | Article Recommendations | Supporting Information

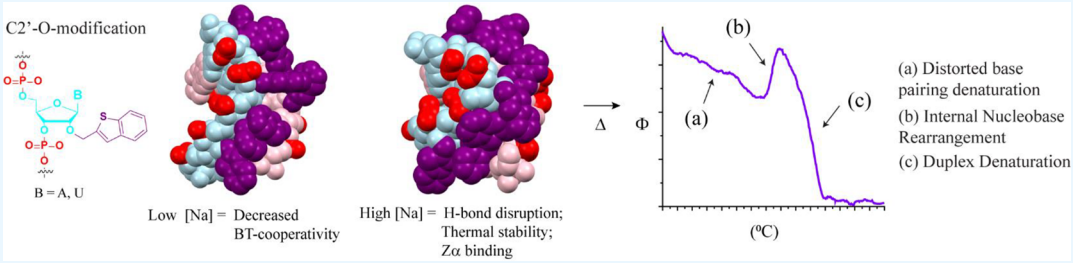

ABSTRACT: Oligonucleotides can be chemically modified for a variety of applications that include their use as biomaterials, in therapeutics, or as tools to understand biochemical processes, among others. This work focuses on the functionalization of oligonucleotides of RNA and DNA (12- or 14-nucleotides long) with methylbenzothiophene (BT), at the C2′-O-position, which led to unique structural features. Circular dichroism (CD) analyses showed that positioning the BT units on one strand led to significant thermal destabilization, while duplexes where each strand contained 4-BT rings formed a distinct arrangement with cooperativity/interactions among the modifications (evidenced from the appearance of a band with positive ellipticity at 235 nm). Interestingly, the structural arrays displayed increased duplex stabilization (>10 °C higher than the canonical analogue) as a function of [Na^+] with an unexpected structural rearrangement at temperatures above 50 °C. Density functional theory−polarizable continuum model (DFT-PCM) calculations were carried out, and the analyses were in agreement with induced structural changes as a function of salt content. A model was proposed where the hydrophobic surface allows for an internal nucleobase rearrangement into a more thermodynamically stable structure, before undergoing full denaturation, with increased heat. While this behavior is not common, B- to Z-form duplex transitions can occur and are dependent on parameters that were probed in this work, i.e., temperature, nature of modification, or ionic content. To take advantage of this phenomenon, we probed the ability of the modified duplexes to be recognized by Zα (an RNA binding protein that targets Z-form RNA) via electrophoretic analysis and CD. Interestingly, the protein did not bind to canonical duplexes of DNA or RNA; however, it recognized the modified duplexes, in a [monovalent/divalent salt] dependent manner. Overall, the findings describe methodology to attain unique structural motifs of modified duplexes of DNA or RNA, and control their behavior as a function of salt concentration. While their affinity to RNA binding proteins, and the corresponding mechanism of action, requires further exploration, the tunable properties can be of potential use to study this, and other, types of modifications. The novel arrays that formed, under the conditions described herein, provide a useful way to explore the structure and behavior of modified oligonucleotides, in general.

INTRODUCTION

Oligonucleotides can be chemically modified for a variety of purposes and have shown great potential in therapeutic applications[1,2] or in the development of aptamer technologies,[3] among many others. In fact, a new family of oligonucleotide-based polymers, in xeno-nucleic acids (XNAs),[4] has been an area with constant developments. Modifications can be incorporated, or designed, at one or more components within the biopolymer, i.e., at the nucleobase, along the phosphate backbone, or on the ribose.[5] Of particular relevance to the present work are reported C2′-O-modifications containing an aromatic ring, some of which include pyrene,[6] thiophene,[7] coronene,[8] perylene,[9] benzyl, and methyl-4-pyridine,[10] with applications that take advantage of increased fluorescence, as strand invaders, or in the design of small interfering RNAs, among others. Furthermore, alkyl groups such as trifluoromethylthio,[11] or methyl,[12] have been used to impart chemical stability, as useful probes to determine RNA structure, or to explore/study biological

Received: July 28, 2022
Accepted: October 7, 2022
Published: October 15, 2022

processes. In this work, we used circular dichroism (CD) to explore the impact that methylbenzothiophene has on the structure of duplexes of RNA and used density functional theory (DFT), together with the polarizable continuum model (PCM), to rationalize the experimental results. We were motivated by previous results,[7] where modification of strands of RNA with methylthiophene groups increased the stability of duplexes of RNA, as long as each strand was modified with four rings, while retaining their ability to fold into A-form double-stranded helices that are typical of canonical RNA:RNA hybrids. Thus, we aimed to increase the thermal stability of the modified duplexes by a slight increase in the size of the aromatic rings, to benzothiophene; however, a distinct behavior was observed that led to unique duplex structures, evident from measurements carried out using CD spectroscopy. Furthermore, the thermal stabilization/destabilization of the novel duplexes was found to be dependent on the concentration of monovalent and divalent cations present in solution. These changes prompted us to explore their ability to bind the Zα-protein, known to target Z-form duplex structures and present within the adenosine deaminase acting on the RNA (ADAR) family.

The work herein describes structural changes on the C2′-modified duplexes that are significant and that lead to distinct alterations in thermal stability as well as in their interactions with proteins. Thus, it is important to understand how certain modifications affect the structure of oligonucleotides at local, within the vicinity of the modification, and global levels. Detailed reviews that focus on structural parameters on the backbone, and not on the base pairing or base stacking, provide a comprehensive explanation for canonical[13] and modified duplexes.[14,15] Of relevance to this work are those located at the C2′-position; for example, the presence of 2′-methoxy modifications in DNA shifts the sugar conformation to N-type, and the interactions between adjacent methyl modifications play a minor role. In addition, the hydrophobicity imparted by the methyl group does contribute to the overall thermal stabilization, typically observed on duplexes containing this functional group.[16] Furthermore, increasing the length of the alkyl chain leads to a decrease in the thermal stability of a DNA:RNA duplex and does not significantly disrupt the hybridization process, forming the expected B- or A-form geometry unless the alkyl chain is increased to nine carbons.[17] The same work described the benzyl group, closest in size to the BT modification used herein, where the presence of one modification led to thermal destabilization; other studies using the benzyl group focused on its potential therapeutic applications and not its impact on the ON structure.[18] The other groups with a similar size or functional group physical properties are (1) methylpyrene, which occupies different environments as a function of the duplex type, i.e., DNA:DNA, DNA:RNA, or RNA:RNA,[6] without affecting the overall formation of B-form or A-form duplexes;[19] and (2) methylthiophene, which increases the duplex stability in a position-dependent manner, arising from conformational changes on the ribose ring and along the phosphate backbone.[20] While there are some detailed reports on the impact that C2′-O-modifications have on the overall structure of RNA, the behavior that is reported herein could not be solely explained, or compared, to these. This work details, and provides rationalization of, the unique structural features and parameters that were obtained as a function of salt content and number/position of the corresponding modifications within the duplexes. Thus, exploring other modified oligonucleotides, while varying the conditions described herein, will be useful for the design and discovery of functional materials or in the structural control of functionalized oligonucleotides (which offer a vast promise in therapeutic applications).

METHODS

General. The procedures, along with full characterization, of all synthetic intermediates that yielded the phosphoramidites used in this work are included within the Supporting Information (pp S3−S16, Figures S1−S20). All water used in the oligonucleotide work was RNase-free, via treatment with diethyl pyrocarbonate.

RNA Synthesis. Oligonucleotides were synthesized on a 394 ABI DNA synthesizer using CPG supports and 2′-*O*-TBDMS phosphoramidites of U, A, C, G, and their corresponding deoxy-analogues dA, T, dC, and dG (all purchased from Glen Research). 0.25 M 5-Ethylthio-1*H*-tetrazole in acetonitrile was used as the coupling reagent; 3% trichloroacetic acid in dichloromethane was used for detritylation; a 2,6-lutidine/acetic anhydride solution was used for capping; and an iodine (0.02 M) in/THF/pyridine/water solution was used in the oxidation step (also purchased from Glen Research). Coupling times of 10 min were used in all cases. Oligonucleotides (ONs) were deacetylated/debenzoylated/deformylated and cleaved from the CPG support in the presence of 1:1 aq. methylamine (40%) and aq. ammonia (40%) with applied heat (60 °C, 1.5 h). A mixture of *N*-methylpyrrolidinone/triethylamine/HF (3:2:1) was used for deprotection of the TBDMS groups (60 °C, 1 h) followed by purification via electrophoresis (20% denaturing PAGE). C18-Sep-Pak cartridges were used to desalt the purified oligomers using 5 mM NH_4OAc as the ion exchange buffer, followed by concentration under reduced pressure. Oligonucleotides were dissolved in H_2O and used as obtained for subsequent experiments. All oligonucleotides were quantified via UV−vis and used without further purification.

RNA Characterization (MALDI-TOF). Samples to obtain mass spectra (MALDI-TOF MS) for all the modified oligonucleotides were prepared as described elsewhere (see acknowledgments and Supporting Information).[21] Mass spectra of all ONs can be found within the Supporting Information (pp S17−S21, Figures S21−S25).

UV−vis Spectroscopy. Concentrations of all oligonucleotides were obtained via UV−vis, using a 1 mm path-length with 1 μL volumes (Thermo Scientific Nano Drop Nd-1000 UV−vis spectrometer). Spectra of all small molecules were obtained using a PerkinElmer Lambda 365 UV−vis spectrophotometer using quartz cuvettes with a 1 cm path length. Origin 9.1 was used to plot the spectra of monomers and oligonucleotides for comparison (see ref 21 for a detailed procedure).

Circular Dichroism (CD) Spectroscopy and Thermal Denaturation Transitions (T_m). CD spectra were recorded at various temperatures (PTC-348W1 Peltier thermostat) using Quartz cuvettes with a 1 cm path length. Spectra were averaged over three scans (350−200 nm, 0.5 nm intervals, 1 nm bandwidth, 1 s response time) and background corrected with the appropriate buffer or solvent. Solutions of RNA always contained sodium phosphate (10 mM, pH 7.2), while the concentration of NaCl, $NaClO_4$, or $MgCl_2$ was varied. All solutions used to record thermal denaturation transitions (T_m) were hybridized prior to recording spectra by heating to 90 °C followed by slow cooling to room temperature (1−2 h). T_m values were recorded at 265, 245, or 235 nm with a ramp of 1°/min and a step size of 0.2 with temperature ranges from 4 to 95

https://doi.org/10.1021/acsomega.2c04784
ACS Omega 2022, 7, 37782−37796

Scheme 1. Synthesis of Modified Oligonucleotides[a]

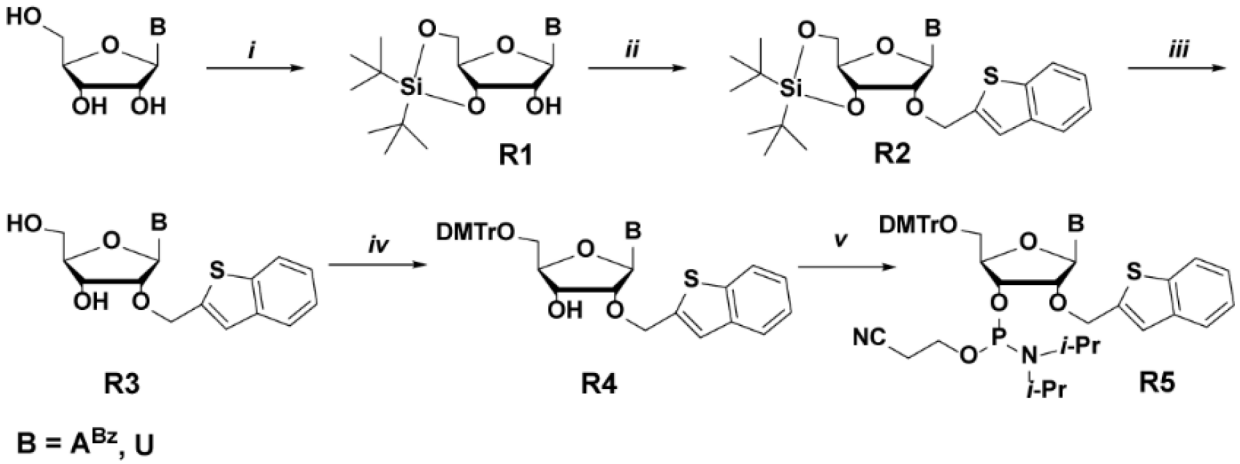

[a] *i.* di-*t*-butyldichlorosilane, imidazole, DMF, 90%; *ii.* NaH, THF/DMSO, BT-methylbromide, 35-75%; 3HF·Et_3N, THF, 80-95%; *iii.* DMTr-Cl, pyridine, 90%; *iv.* OCE-diisopropylamine phosphonamidic chloride, DIPEA, DCM, 90%.

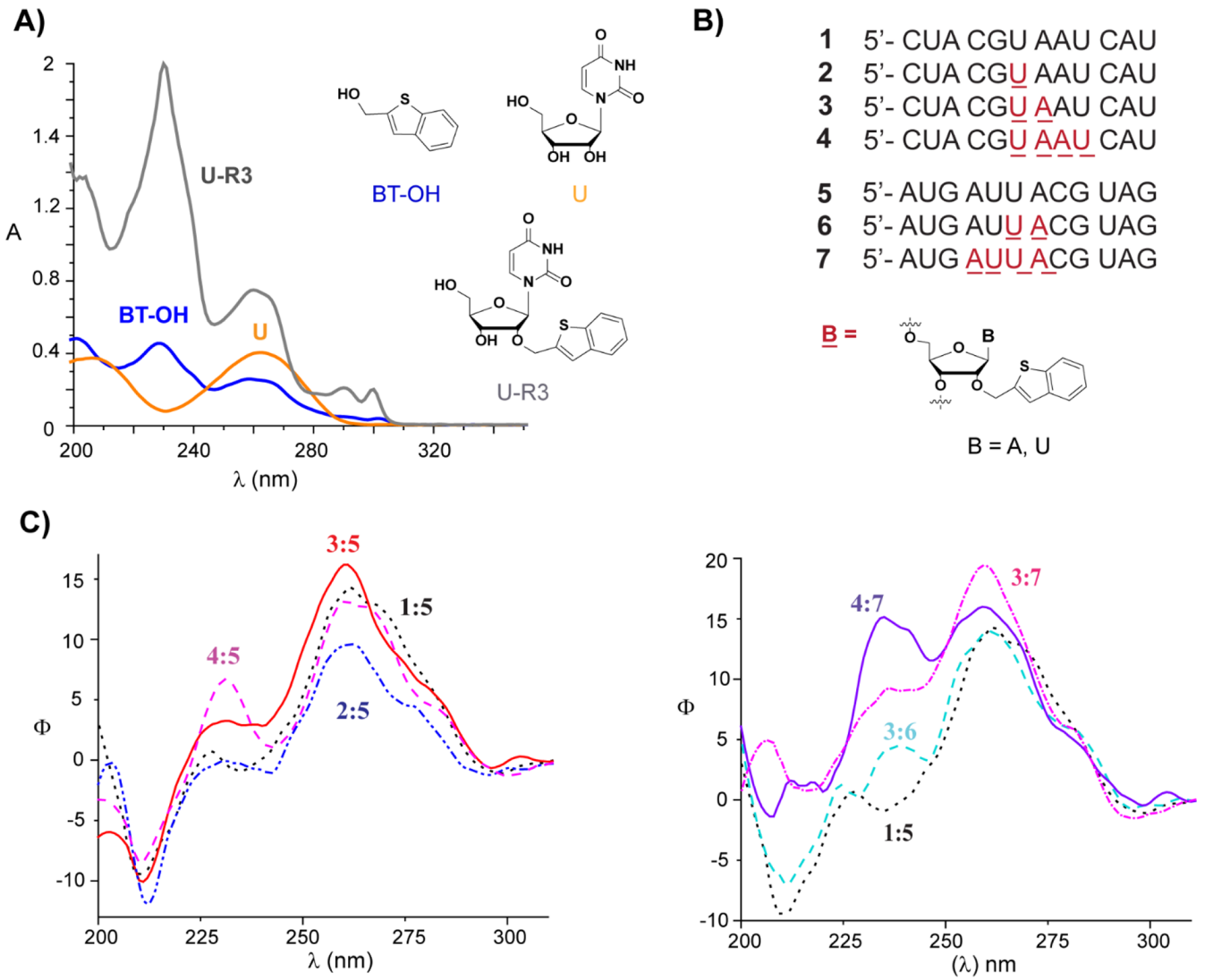

Figure 1. (A) UV−vis spectra of benzothiophene-2-methanol, uridine, and modified uridine R3, taken in a 1:1 mixture of MeOH/H_2O at 300 μM concentrations, 1 mm path length; (B) sequence of canonical and modified oligonucleotides **1**−**7**. (C) CD spectra at room temperature (rt) using the conditions described in Table 1.

https://doi.org/10.1021/acsomega.2c04784
ACS Omega 2022, 7, 37782−37796

°C. A thin layer of mineral oil was added on top of each solution to keep concentrations constant at higher temperatures. Origin 9.1 was used to determine all T_m values and to generate all figures.

Zα-Protein. The protein was a gift from Prof. Quentin Vicens, Prof. Beat Vögeli, and Parker Nichols, expressed as described previously[22] and diluted (4.2 mM) in a potassium phosphate (20 mM, pH 6.4)/sodium chloride (20 mM) solution.

Circular Dichroism in the Presence of Zα. All duplexes were hybridized as mentioned above. Each duplex solution was then distributed into two different cuvettes (160 μL each), followed by recording of the CD spectra. The solutions were then titrated with the protein solution (2 or 3 μL, 560 μM in 4.7 M NaCl, 100 mM sodium phosphate, pH 7.2) or buffer (2 or 3 μL, 4.7 M NaCl, 100 mM sodium phosphate, pH 7.2), followed by incubation for 20 min. CD spectra were recorded after each protein-buffer addition, and the process was repeated 2−3 times. T_m measurements were carried out, following the titrations, as described above.

Oligonucleotide 5′-^{32}P-Radiolabeling. Oligonucleotides were radiolabeled by mixing polynucleotide kinase (PNK), PNK buffer, ATP, RNA, and water (final volume = 50 μL) according to manufacturer's procedure followed by heating to 37 °C for 45 min. Radiolabeled materials were passed through a G-25 sephadex column followed by purification via electrophoresis (20% denaturing PAGE). The bands of interest (slowest) were extruded and eluted over a phosphate saline buffer solution (10 mM NaCl, 10 mM Na_3PO_4, pH 7.2) for 12 h at 37 °C. The remaining solution was filtered and concentrated to dryness under reduced pressure followed by precipitation over NaOAc and ethanol. The supernatant was removed, and the remaining oligonucleotide was dried and redissolved in water. Activity was assessed using a Beckmann LS 6500 scintillation counter.

RESULTS

Synthesis of Modified Oligonucleotide. Ribonucleosides were modified at the C2′-O-position with 2-methylbenzothiophene groups and transformed to their corresponding phosphoramidites (Scheme 1) for their incorporation into oligonucleotides of RNA or DNA, via solid-phase chemistry. Uridine and adenosine were chosen, for derivatization, given that the pyrimidine nucleoside does not require the addition of protecting groups to the nucleobase. Both were functionalized by using their corresponding 5′,3′-di-*t*-butyl silyl derivatives (**R1**) in the presence of sodium hydride and 2-bromomethylthianaphthene, to afford the corresponding protected nucleosides in varying yields (**R2**). Alkylation of the uridyl nucleoside resulted in lower yields, where the formation of suspensions was typically observed, and adjusting the concentration or temperature did not lead to enhanced yields. Bromination of benzothiophene methyl alcohol was achieved via an Appel reaction following a known procedure.[23] Deprotection in the presence of HF yielded diol **R3** in good yields, which was tritylated under standard conditions to afford nucleosides **R4**. Subsequent phosphytilation, under standard conditions afforded their corresponding phosphoramidites (**R5**). Full details for the synthesis and characterization of both phosphoramidites are included within the Supporting Information (pp S3−S16, Figures S1−S20).

The photophysical behavior of modified nucleoside (**U-R3**) was compared to that of benzothiophene-2-methanol and uridine (Figure 1A). As expected, the modified nucleoside displayed two bands (λ_{max} = 230 and 260 nm) that matched those observed for uridine and benzothiophene-2-methanol. In addition, a band with a lower extinction coefficient and absorption at a higher wavelength was observed for the modified nucleoside (λ_{max} = 285 and 300 nm) and can be assigned to the presence of the benzothiophene ring.[24]

RNA Duplex Structure and Stability. The sequence of the RNA dodecamers was chosen such that the oligonucleotides contained U or A in the central region while yielding thermally stable duplexes (Figure 1B, ONs **1**−**7**), which allowed us to systematically explore the impact of 1−4 modifications on both strands, under various conditions. Circular dichroism (CD) was used to track the presence/formation of secondary structure, identify changes within the expected A-form duplexes, and determine their thermal stability. All thermal denaturation transitions (T_m) were obtained by monitoring the change in intensity of the dichroic signal, at the lambda max (260 or 235 nm), as a function of increased heat. The initial conditions included the presence of standard mono- and divalent cationic salts (NaCl and $MgCl_2$) in sodium phosphate buffered solutions (pH 7.2). Formation of an A-form duplex was confirmed, via circular dichroism (CD), upon hybridization of both complementary/canonical strands **1** and **5**, where bands with a maximum at 260 nm and a minimum at 210 nm were observed (Figure 1C). The trace for the T_m displayed a sigmoidal curve indicating a denaturation transition at approximately 62 °C (Table 1, entry 1 and Figure S27). As illustrated, the incorporation of 1−4 benzothiophene (BT) units on one strand also presented features of an A-form duplex while displaying decreased T_m values as a function of the number of aromatic probes present (**1**:**5**−**4**:**5** and **1**:**6**−**1**:**7**, Tables 1 entries 1−6). Sharp transitions were evident from the sigmoidal shapes observed for up to 0−2 incorporations on one strand (**1**:**5**−**3**:**5**), while the presence of four BT units (**4**:**5**) led to the appearance of two transitions (Figure S27). The impact of the BT units on RNA duplexes, when present on both strands, was explored next, where the appearance of two transitions and the lack of a clear sigmoidal shape was obtained in some cases (Table 1, entries 6−11; Figure S27). Interestingly, incorporation of six or more benzothiophene units on both strands led to the disappearance of the band at 210 nm which is used to assign the formation of an

Table 1. Thermal Denaturation Transitions of All Possible Duplex Combinations, Recorded at 260 nm[a]

entry	duplex	T_m	T_{m2}
1	1:5	62.5 ± 0.4	
2	2:5	59.2 ± 2.1	
3	3:5	56.1 ± 1.2	
4	4:5	47.1 ± 5.6	23.4 ± 2.6
5	1:6	55.4 ± 0.6	
6	1:7	47.1 ± 1.1	26.1 ± 1
7	2:6	50.9 ± 1.6	< 33
8	2:7		25.1 ± 0.6
9	3:6	54.4 ± 2.4	< 28
10	3:7		< 24
11	4:7		< 25

[a]All measurements were carried out in triplicate. Samples of all traces are provided within Supporting Information (Figure S26); entries with a < sign did not display a clear sigmoidal shape. [RNA duplex] = 2.5 μM, [NaCl] 10 mM, [$MgCl_2$] = 5 mM, [Na_3PO_4] = 10 mM, pH 7.2.

https://doi.org/10.1021/acsomega.2c04784
ACS Omega 2022, 7, 37782−37796

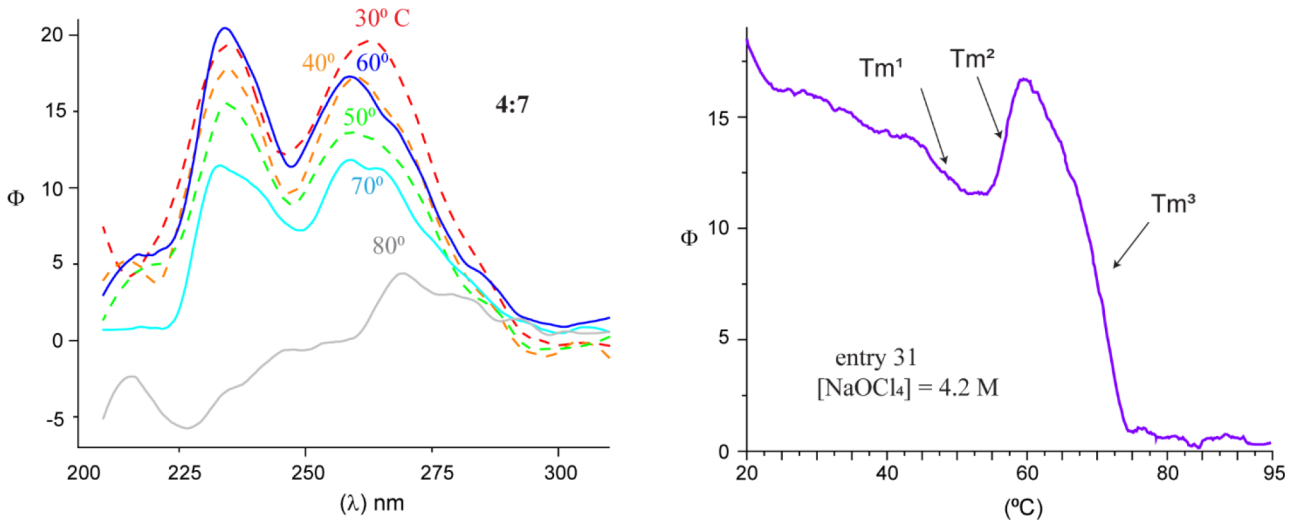

Figure 2. CD spectra at various temperatures of modified duplex **4:7** at [$NaClO_4$] = 4.2 M (left) and T_m trace recorded at 260 nm (right). All experiments contained 10 mM sodium phosphate at pH 7.2 and NaCl (10 mM).

Table 2. Thermal Denaturation Transitions of Duplex 4:7, Recorded at 260 nm[a]

duplex 1:5				duplex 4:7				
entry	[NaCl]	[$MgCl_2$]	T_m	entry	[NaCl]	[$MgCl_2$]	T_m	T_{m2}
12	10 mM		39.7 ± 0.7	**19**	10 mM		< 30	
13	100 mM		47.6 ± 0.5	**20**	100 mM		42.9 ± 0.6	
14	820 mM		57.2 ± 0.4	**21***	700−800 mM		65.4 ± 0.9	
				22*	1.1		57.2 ± 1.2	72.6 ± 0.5
15	4.3 M		58.6 ± 0.5	**23**	4.1 M		55.1 ± 01.5	
				24	10 mM	5 mM	< 30	
16	100 mM	5 mM	61.6 ± 0.5	**25**	100 mM	5 mM	31 ± 0.8	
17	650−800 mM	5 mM	60.2 ± 0.8	**26**	650−800 mM	5 mM	28.2 ± 1.1	
18	3.5−4.2 M	5 mM	55.2 ± 0.6	**27**	3.5 M	5 mM	nd	

[a]All measurements were carried out in duplicate. Samples of all traces are provided within Supporting Information (Figures S27−S30); entries with a < sign did not display a clear sigmoidal shape. [RNA duplex] = 2.5 μM, [Na_3PO_4] = 10 mM, pH 7.2. Entries with a (*) indicate instances that display increased thermal stability, compared to the canonical analogue.

A-form duplex, along with a concomitant appearance of a distinct band with positive ellipticity at 235 nm (Figure 1C). There were two unexpected observations: (1) the band at 235 nm exhibited a comparable molar ellipticity as the band with λ_{max} at 260 nm; and (2) the thermal stability was lower (entries 10−11), and with T_m traces that did not display a clear sigmoidal shape (which differed from a previous report using thiophene[7]). Based on this CD spectra, two possibilities were considered: (1) cooperative $\pi-\pi$ stacking, or other interactions, among benzothiophene units; or (2) formation of a Z-form-like duplex, albeit with bands at different wavelengths (*vide infra*).

Given that the CD spectra displayed significant differences, as more BT units were incorporated, and that different duplex forms led to unique spectroscopic features, we considered the formation of a distinct duplex. On this note, the formation of a Z_R-duplex is characterized by the appearance of two bands with positive ellipticity at 285 and 255 nm, which is similar to that observed for duplex **4:7**, albeit with a hypsochromic shift of ca. 20 nm for both bands (Figure 2C). In addition, the formation of different duplex forms has been reported to depend on different factors such as temperature,[25] salt content, or chemical modifications at the nucleobase[26,27] or backbone.[28] Thus, we set out to explore the effect of [Na^+] in the presence and absence of one of the most common divalent cations known to interact with nucleic acids, Mg^{2+}. Increasing the [Na] in the absence of a divalent cation increased the thermal stability of the canonical duplex **1:5** (Table 2, entries 12−15) in the range between 10 mM and 4 M. On the other hand, all denaturation transitions values decreased in the presence of Mg (Tables 1 and 2, entries 1, 16−18). To further explore the impact of the monovalent cation, we decided to use sodium perchlorate ($NaClO_4$), which is a salt that can induce the formation of a Z-form duplex. Thermal denaturation transitions of the canonical duplex resulted in similar trends as those obtained in the presence of NaCl (Table S1), and all conditions displayed features consistent with an A-form duplex. The experiments validated the use of this salt without a significant impact on thermal stability, unless high $NaClO_4$ concentrations were used (entries S4 and S8), where a significant destabilization was observed in the presence/absence of $MgCl_2$. Equivalent experiments were then carried out on the modified duplex **4:7**, where the formation of the two bands with positive ellipticity was observed in all cases. However, the presence of magnesium resulted in a sharp structure destabilization with T_m traces showing poor sigmoidal curves (entries 24−27, Figure S31). On the other hand, removal of magnesium led to increased thermal stability as a function of increased [NaCl] in the range from 10 mM to 0.8 M (entries 19−21). Interestingly, increasing the [NaCl] to 1 M displayed two T_m transitions with one showing increased thermal stabilization of approximately 7 °C (entry 22, Figure

https://doi.org/10.1021/acsomega.2c04784
ACS Omega 2022, 7, 37782−37796

Table 3. Thermal Denaturation Transitions of Duplex 4:7, Recorded at 260 and 235 nm[a]

entry	[$NaClO_4$]	$Tm_{260}{}^1$	$Tm_{260}{}^2$	$Tm_{260}{}^3$	$Tm_{235}{}^1$	$Tm_{235}{}^2$	$Tm_{235}{}^3$
28	10 mM	< 30			nd		
29	100 mM	45.6 ± 0.3			45.7 ± 0.3		
30*	1 M	63.2 ± 0.5			45.2 ± 0.6	59.8 ± 1.1	
31*	4.2 M	46.4 ± 3.1	59.3 ± 1.4	73.1 ± 1	49.8 ± 3.6	59.7 ± 1	73.1 ± 1.3

[a]All measurements were carried out in duplicate, in the absence of Mg^{2+} containing [NaCl] = 10 mM and sodium phosphate (10 mM, pH 7.2). Entries with a (*) indicate instances that display increased thermal stability, compared to the canonical analogue.

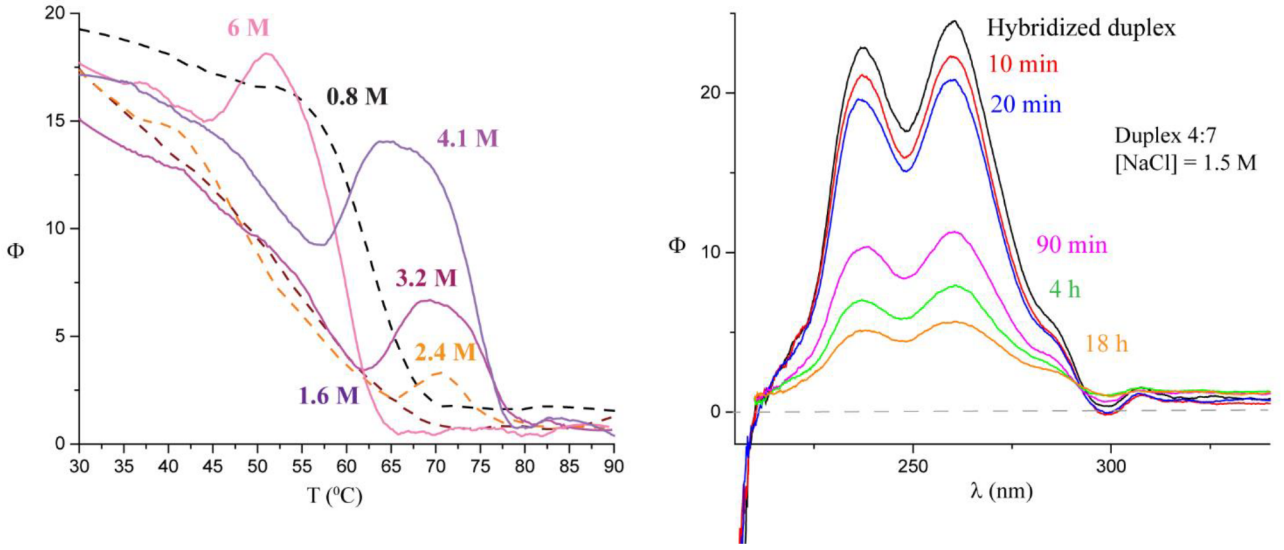

Figure 3. Thermal denaturation transitions of modified duplex **4:7** at varying [$NaClO_4$] (left); and duplex stability as a function of time and [NaCl], incubated at room temperature for 18 h (right). All experiments were carried out in the presence of 10 mM sodium phosphate at pH 7.2.

S30) with respect to its canonical analogue. Concentrations of sodium chloride higher than 1.1 M also led to destabilization (entry 23). It is worth noting that the values did not vary when measuring the changes in ellipticity, as a function of temperature, at either of the wavelength maxima (260 or 235 nm). This provided a clear indication that increasing the NaCl content increased stability and that the presence of Mg^{2+} destabilizes the BT-modified duplex formation, presumably from interactions occurring with the benzothiophene ring. We then carried out the corresponding experiments using duplex **4:7** in the presence of $NaClO_4$ (Table 3). The presence of the divalent cation Mg^{2+} led to significant destabilization in all cases and is not shown/discussed herein. As in the case of the canonical duplex, T_m values increased, as a function of increased [$NaClO_4$], from less than 30 °C at 10 mM to 63 °C at 1 M (entries 28−30). Unexpectedly, increasing the concentration to approximately 4 M led to a supramolecular transformation with two denaturing transition values at $T_m{}^1$ 46 and $T_m{}^3$ 73 °C, along with a stabilizing rearrangement $T_m{}^2$ value at 59 °C (entry 31 and Figure 2). The same behavior was observed upon measuring the T_m at 235 nm.

In light of these results, we decided to explore this structural rearrangement in more detail by measuring the thermal denaturation transitions of the modified duplex as a function of [$NaClO_4$]. Interestingly, the behavior of duplex **4:7** was highly dependent on this factor (Figure 3), where the denaturation trace at 0.8 M showed a single T_m transition at approximately 63 °C; however, increasing the concentration to 1.6 M displayed a depressed, and broadened, denaturation trace with a T_m value < 54 °C. Notably, further increments in the sodium perchlorate concentrations, to 2.4 M, led to the appearance of the high-temperature conformational rearrangement, albeit with a transition that was not as pronounced. The intensity of the band, assigned to this supramolecular transition, increased as a function of [$NaClO_4$], where the most stable structure was observed at 4.1 M. Further increments, to 6 M, led to a depressed T_m, with the main denaturing transitions changing from 73 to 60 °C. The fact that CD spectra obtained at varying temperature leads to an increase in the band at 235 nm (Figure 2, compare CD spectra at 30° and 60 °C) suggests that the benzothiophene rings play a major role in this behavior.

To rule out a potential reaction between sodium perchlorate and the benzothiophene rings, where $NaClO_4$ can function as an oxidizer, we probed its reactivity. Gratifyingly, reactions between 2-benzothiophenylmethanol and sodium perchlorate, with heat, lacked any reactivity. The same was observed on the nucleoside containing the benzothiophene probe (**UR3**), where no reactivity was detected via TLC or NMR. This provides indication that the integrity of the aromatic unit, or nucleobases, is not compromised under the conditions explored in this work.

Upon reproducing experiments, we were surprised to observe that the intensity of the signals for duplex **4:7** diminished as a function of time. However, this was only observed at high salt concentrations (Figure 3), where the intensities were partially recovered upon heating. This suggests that the high concentration of sodium ions may affect the duplex stability, although it is unclear why the overall dichroic shape of the duplex is not lost. Interestingly, there is no evidence that denaturation to the corresponding single-stranded modified RNAs is occurring but rather that the [NaCl] may be inducing aggregation or other type of behavior among the corresponding duplex structures. On the other hand, solutions prepared at a lower [NaCl] did not

https://doi.org/10.1021/acsomega.2c04784
ACS Omega 2022, 7, 37782−37796

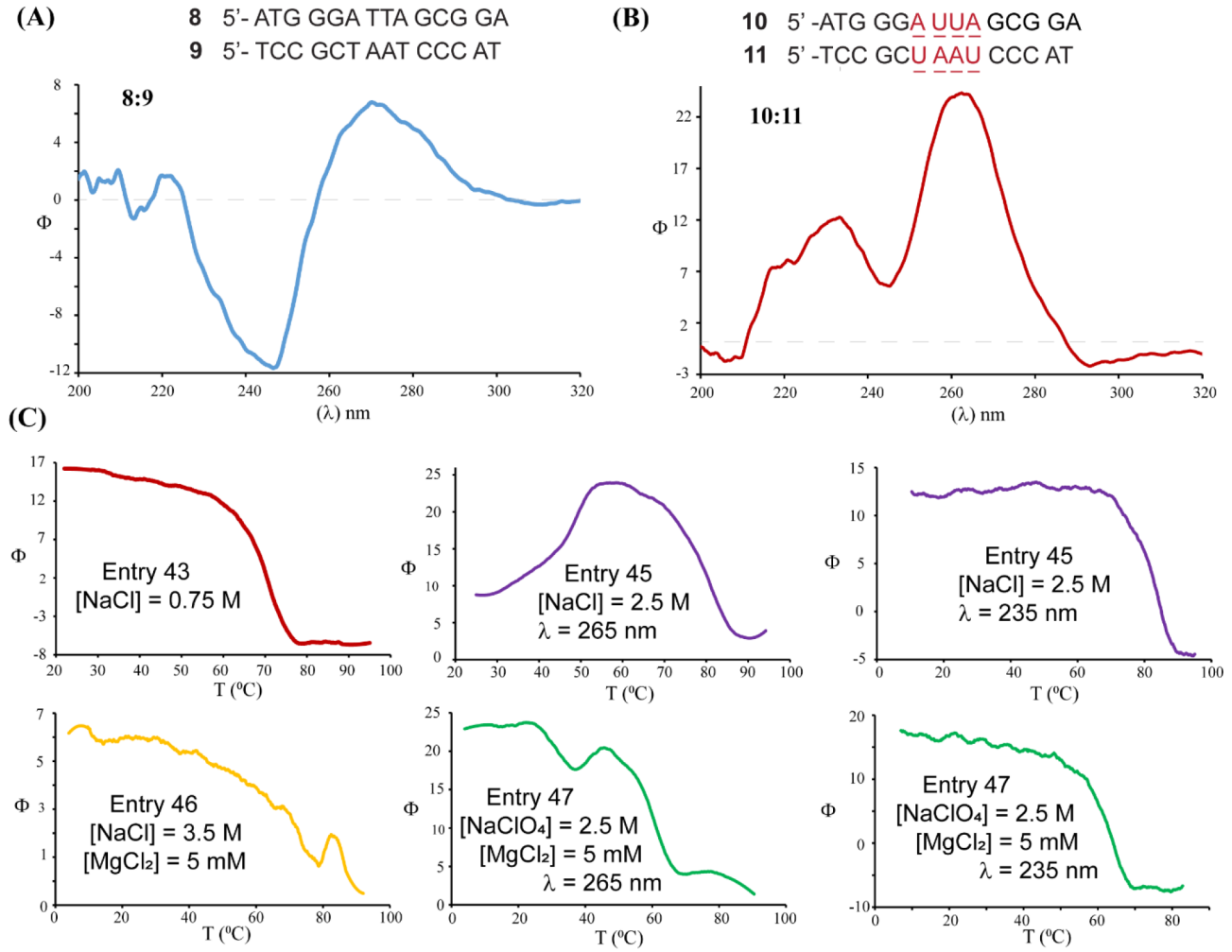

Figure 4. (A) Representative CD spectrum and T_m of canonical B-form duplex **8**:**9** along with all obtained values; (B) representative CD spectrum of BT-modified duplex **10**:**11** along with all obtained values; and (C) T_m measurements of BT-modified duplex **10**:**11** in various conditions. All experiments were carried out in triplicate, in the presence of 10 mM sodium phosphate at pH 7.2.

show any difference as a function of time, in experiments tracked up to 5 days (Figure S32)

DNA Duplex Structure and Stability. In order to probe the potential impact arising from the C2′-OH groups, where it has been well established that RNA A-form duplexes have a smaller rise (shorter duplex) and inclination, compared to its analogous B-form duplex,[29] we decided to incorporate the BT-modified nucleosides into complementary tetradecamers containing deoxynucleotides at the 5′- and 3′-regions (Figure 4A). The length and sequence were varied, compared to the RNA analogues, to increase thermal stability of the canonical duplex and ensure thermal denaturation transitions higher than approximately 50 °C. As expected, the canonical duplex **8**:**9** displayed features that were consistent with a B-form duplex, mainly two bands with positive and negative ellipticity at approximately 265 and 245 nm, respectively. Applying heat led to the disappearance of the band at 245 nm and allowed us to measure the corresponding thermal denaturation transitions while varying the salt content, with all curves showing a distinct sigmoidal transition. The thermal stability of the canonical duplex (**8**:**9**) was unaffected by increased [NaCl] in the presence of Mg^{2+} (entry 32). However, removing the dimetal cation led to decreased thermal stability at lower [NaCl] (entry 33), no effect at [NaCl] between 0.7 and 2.5 M (entry 34), and decreased thermal stability at higher [NaCl] (entry 35). Interestingly, substituting the ionic content for sodium perchlorate led to overall thermal destabilization of the duplexes, with a maximum stability at approximately 1 M and decreasing stability as the [$NaClO_4$] was increased (entries 36−39). We then explored the structural thermal rearrangement formed by duplex **10**:**11**, which contained four benzothiophene units on each strand located within the midregion of the duplex. As with the BT-RNA duplex **4**:**7**, the CD spectra displayed two bands with positive ellipticity at 265 and 235 nm (band with negative ellipticity at 245 nm—from canonical duplex—was abolished) (Figure 4B). This suggests that the benzothiophene units are, possibly, on the periphery of the duplex and that π—π, or other, interactions among them are likely to be in place. Interestingly, measurement of the thermal denaturation transitions led to a different behavior with respect to the canonical duplex, as well as when the ionic content was varied. Low sodium and magnesium concentrations displayed structure destabilization (entry 40), while increasing the [NaCl] in the 0.1−2 M range increased stabilization of the duplex significantly, displaying a lower T_m value than its canonical analogue (entries 32 and 41). Furthermore, increasing the salt content above 2 M in NaCl led to significant stabilization, along with the appearance of a second transition, potentially assigned to ordering/arrangement

https://doi.org/10.1021/acsomega.2c04784
ACS Omega 2022, 7, 37782−37796

Table 4. Thermal Denaturation Transitions of Duplex 8:9 or 10:11, Recorded at 260 nm[a]

duplex 8:9				duplex 10:11				
entry	[$MgCl_2$]	[NaCl]	T_m	entry	[$MgCl_2$]	[NaCl]	T_m	T_{m2}
32	5 mM	0.01−3.6 M	64.6 ± 1.1	**40**	5 mM	10 mM	33.8 ± 0.7	
33		10 mM	46.1 ± 0.7	**41**	5 mM	0.1−2 M	59.4 ± 2.4	
34		0.7−2.5 M	65.7 ± 0.8	**42***	5 mM	2.5−4.7 M	76.1 ± 3.1	86.1 ± 1.1
35		3.6 M	62.5 ± 0.5	**43***		0.75 M	69.6 ± 0.9	
				44*		1.5 M	74.1 ± 0.3	
				45*		2.5 M	48.9 ± 0.3 ↑	79.6 ± 2.1
				46*		3.5 M	46.3 ± 0.3 ↑	> 80
		[$NaClO_4$]				[$NaClO_4$]		
36		0.1 M	56.1 ± 1.3	**47**	5 mM	0.1−2.5 M	34.1 ± 3.9 ↓	62.3 ± 2.2
				48	5 mM	4.7 M	23.1 ± 9.6	51.9 ± 0.6
37		1 M	59.3 ± 0.8	**49***		1 M	64.7 ± 0.7	
38		2.7 M	45.2 ± 1.1	**50***		2.7 M	61.8 ± 0.6	
39		5.4 M	21.8 ± 1.8	**51***		5.4 M	50.1 ± 0.5	

[a]All measurements were carried out in duplicate, in the absence of Mg. Entries with a (*) indicate instances that display increased thermal stability, compared to the canonical analogue.

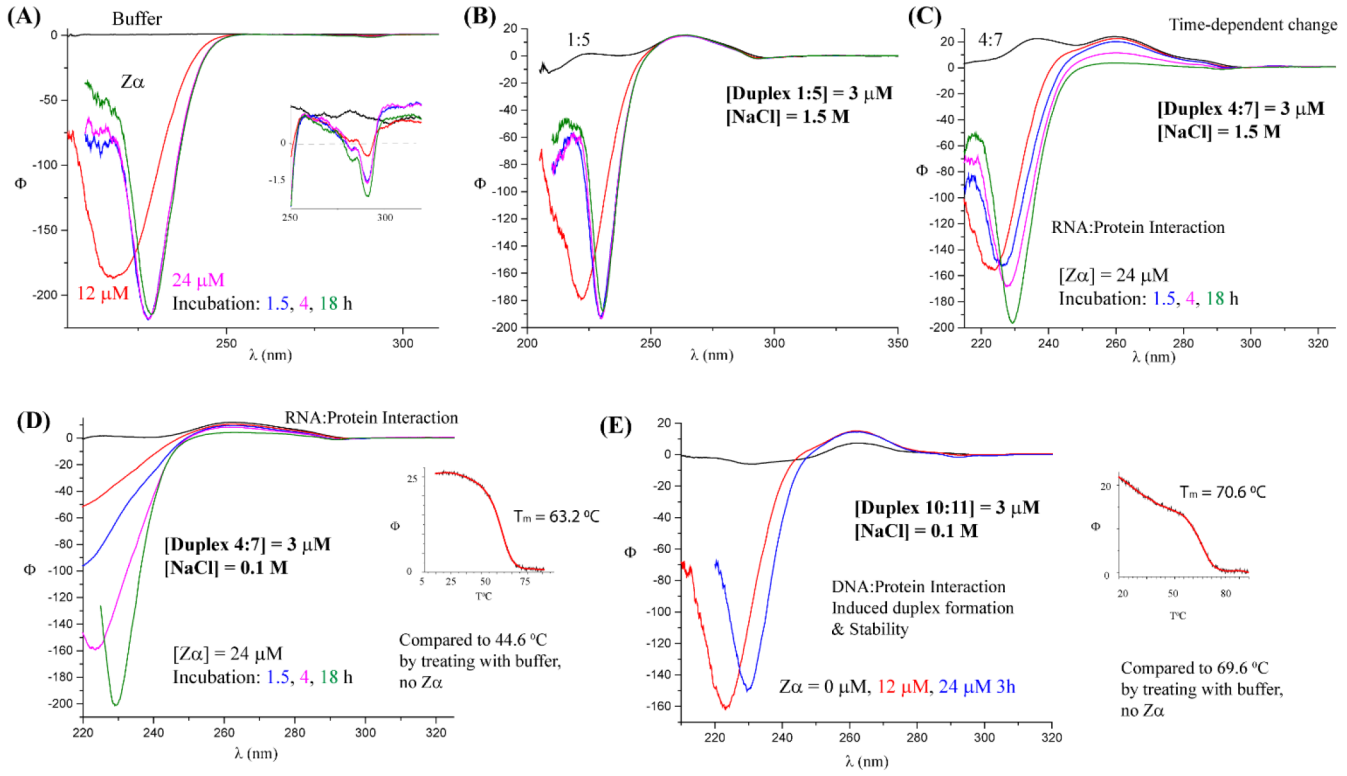

Figure 5. CD spectra corresponding the (A) Z*α*-protein titrated with buffer, (B) duplex **1:5** titrated with Z*α*; (C−D) duplex **4:7** titrated with Z*α* at different [NaCl]; and (E) duplex **10:11** titrated with Z*α*. All RNA/DNA solutions were prepared in 10 mM Na_2PO_4 pH 7.4, and [NaCl] = 0.1 or 1.5 M. Z*α* was prepared fresh in the desired buffer and titrated into the duplex solutions.

among the nucleobases (entry 42 and Figure 4C). Removal of the divalent metal displayed stabilization of approximately 4 °C, up to [NaCl] in the 0.75 M range (entry 43), and approximately 8 °C in the presence of 1.5 M [NaCl] (entries 44). On the other hand, decreasing the [NaCl] to 0.1 M did not display sigmoidal T_m transitions or cooperativity among the benzothiophene rings, *vide infra*. While increasing [NaCl] to 2.5 M led to a more stable, distinct, structure upon addition of heat, the second one showed denaturation of the structure (entries 45 and 46). Monitoring of T_m measurements at different wavelength displayed different curves, where the supramolecular arrangement (observed at 265 nm) disappeared upon recording at 235 nm (Figure 4C, entry 45 example). This observation suggests that the nature of this rearrangement arises from changes within the nucleobases, while the benzothiophene rings may aid in stabilizing the duplex, until the second transition is observed (where full denaturation is recorded). Lastly, we probed the impact of the sodium cation by using $NaClO_4$ as a substitute. In this case, a different T_m trace was obtained, where two denaturing transitions were observed along with a rearrangement to another structure (entries 47 and 48, and Figure 4), carried out in the presence of Mg^{2+}. Removal of the divalent metal, while increasing the $NaClO_4$ concentration, led to traces with one transition, and that yielded

https://doi.org/10.1021/acsomega.2c04784
ACS Omega 2022, 7, 37782−37796

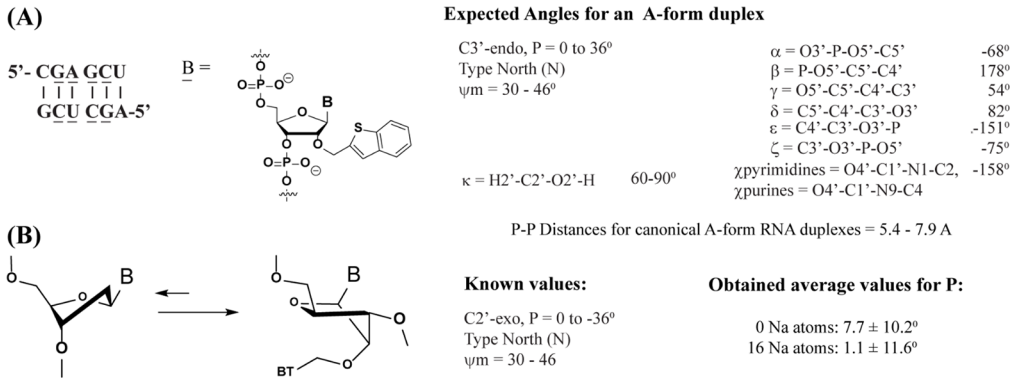

Figure 6. (A) Modified sequence/duplex that was modeled (left); and pseudorotational angle (P), pucker amplitude (ν), and torsion angles expected for an A-form duplex; and (B) obtained values for (P), as a function of added sodium, falling in the range for the C2′-exo conformation (the illustrated average values correspond to averages of all ribose rings at the M06−2X/6G* level).

destabilization as a function of increased perchlorate (entries 49−51).

Probing for a potential effect on the impact arising from time and [Na], solutions of DNA duplexes **8**:**9** and **10**:**11** were prepared under the same buffered conditions as in Figure 3 and incubated over periods of time up to 72 h, with no significant change detectable, via CD. This result points to the stark differences imposed by the 2′-OH, located at both extremes of the duplexes.

RNA/DNA−Protein Interactions. Given the interesting structural properties, and behavior, of the modified duplexes, we decided to probe their potential interaction with an RNA-binding protein. Specifically, we used Zα to probe for binding to the DNA or RNA duplexes. It has been established that this RNA-binding protein targets Z-form duplexes by taking advantage of their disordered nature, arising from torsions around the glycosidic bond within the nucleobases, known to occur at high salt concentrations. Binding to the modified RNA or DNA duplexes, by the protein, would imply some potential disorder within the nucleobases, or attraction to its hydrophobic core. To carry out these experiments, Zα was titrated into canonical and modified duplexes of RNA (**1**:**5** and **4**:**7**) or DNA (**8**:**9** and **10**:**11**), and compared to the corresponding titrations with buffer (as control reactions). Furthermore, thermal stabilities were measured in the presence of the protein (Figure 5). As in previous reports, circular dichroism of the Zα protein (Figure 5A) displayed features consistent with the presence of ß-structures (absorption at 210−220 nm) along with a weaker band arising from the aromatic amino acids (absorption at 280−290 nm).[30]

Duplexes of canonical RNA (**1**:**5**), prepared in higher [NaCl], were treated with 4 and 8 mol equiv of the Zα protein, and their potential interaction was tracked via CD. As illustrated in Figure 5-B, there was no change in the bands at 260 or 220 nm, corresponding to the RNA or protein, respectively, which suggested that no interaction between these biopolymers was present. On the other hand, addition of Zα to the modified RNA duplex (**4**:**7**) resulted in significant changes as follows (Figure 5C): (1) the intensity in the band at 260 nm decreased as a function of time; however, this change may be assigned to that described previously (Figure 3) and does not necessarily indicate binding; and (2) the band associated with the protein displayed changes that indicated potential RNA−protein interactions. Heating of the modified duplex−protein complex (Figure S33E) displayed a hypochromic shift with a major change between 40 and 70 °C, and a major transition between 70 and 80 °C (hyper- and bathochromic shifts), which confirmed that RNA−protein interactions are impacting the thermal stability of the duplex. To probe for a dependence on salt content, experiments at lower [NaCl] were carried out, and consistent with the previous observation, the canonical analogue (**1**:**5**) did not exhibit any change, following Zα addition. On the other hand, titration of Zα into the modified duplex (**4**:**7**, Figure 5D) led to changes in both of the main absorption bands. Since this duplex does not display any change as a function of time, in the absence of protein, the observed change (260 nm) was assigned to the formation of a protein−RNA interaction, a fact that was confirmed by the concomitant change in the band at 220 nm. Furthermore, heating of the sample resulted in a thermal denaturation transition approximately 19 °C higher than the T_m obtained in the absence of the protein (entry 20), suggesting that the Zα binds to the RNA and increases its thermal stability (or that of the protein:RNA complex).

We then carried out the same experiments on the DNA analogues. As expected, there was no evidence of binding to the canonical DNA duplex (**8**:**9**) at a higher salt concentration ([NaCl] = 1.5 M); however, we were surprised to see that the modified duplex **10**:**11** did not show behavior that would be consistent with binding (Figure S33F,G). Taking in consideration that the protein may increase the stability of the duplex, samples at lower salt concentrations were prepared (0.1 M NaCl). Under these conditions, the canonical DNA duplex **8**:**9** forms a stable secondary structure (Figure S33H, entry 33) and did not display features consistent with protein binding. Furthermore, experiments using the modified duplex **10**:**11**, under the same salt content, do not display a structure that involves the benzothiophene rings (Figure S33I). However, its treatment with the Zα-protein led to a substantial hyper-dichroic shift along with a T_m measurement that was in agreement with a sharp thermal stabilization (Figure S33J, entry 43), much like that obtained at higher [NaCl]. This suggests that the enzyme may be inducing (1) the nucleobase rearrangement observed previously, or (2) the cooperativity of the BT rings, that in turn leads to the stabilized structure.

The formation of an oligonucleotide−protein complex was corroborated via electrophoretic analyses (native PAGE). A band that is consistent with a protein−RNA complex was observed with modified duplex **4**:**7** and not with single-stranded RNA **4** (Figure S34A; lanes A−G) nor with the canonical analogues **1** or **1**:**5**. In contrast, experiments on the DNA

https://doi.org/10.1021/acsomega.2c04784
ACS Omega 2022, 7, 37782−37796

analogue showed only complex formation at lower salt concentrations (Figure S34A,C; lanes H/I and L/M), consistent with the obtained results using CD (Figure S33J).

Overall, these observations suggest that this RNA-binding protein has an affinity toward the RNA, or DNA, containing the benzothiophene rings in a salt-dependent manner. This may be due to an affinity to the hydrophobic core of the RNA to the motif within the protein, responsible for binding the RNA duplex; or to a distinct duplex that exposes the nucleobases, for subsequent recognition. In both cases of the modified nucleic acids, the enzyme induced increases in the thermal stability of the duplexes.

MODELING

To gain a better understanding of the impact of (1) the 2-benzothiophenemethyl group at the C2′-*O*-position; and (2) the monocation dependence (sodium in this case) on the structure of the RNA duplexes, modeling was carried out. Density function theory (DFT) calculations were performed with the polarizable continuum model (PCM)[31−33] using the quantum chemical program Gaussian 16.[34] The models and methodology were previously validated[20] and applied toward the benzothiophenyl modified oligonucleotides. For the present DFT-PCM calculations, we employed two functionals, the B3LYP hybrid functional with Grimme's D3 dispersion correction (GC3)[35] and the M06-2S functional.[36] We also used two basis sets in our investigation, the 3-21G* basis set and the 6-31G* basis set, thus resulting in four combinations of theories: B3LYP-GD/3-21G*, B3LYP-GC/6-31G*, M06-2S/3-21G*, and M06-2X/6-31G*. To allow for a direct comparison with previous work, the sequence illustrated on Figure 6 was used. Models from the previous calculations were used and edited to contain a benzothiophene ring at four positions on each strand, followed by application of different levels of theory until the structures converged to a low energy minima. The conclusions described in the text correspond to a reasonably adequate level of theory (M06-2X/6G*) for the molecular systems considered herein. The robustness of our analyses is corroborated by noting the fact that all other theories displayed similar results (B3LYP-GD3/3-21G*, B3LYP-GD3/6-31G*, M06-2X/3-21G*; see Supporting Information Figures S40−S51). For our purposes, the minimum energy structures were used to analyze all angles and rationalize changes in structure overall. To this end, the Altona-Sundaralingam parameters[37] were used to establish structural changes induced by the benzothiophene ring (Figure 6A). Analyses of all structures were carried out by measuring all of the angles of interest and obtaining the average and standard deviation of all measurements, shown within Table 5. Standard deviations greater than 25% of the average value were considered as significant changes, that potentially result in structural outcomes that can relate to the experimental observations (see Figures S40−S51 for tables containing all angle measurements)..

All of the measurements corresponding to a canonical model were reported previously[7] and are in agreement with canonical A-form RNA duplexes as follows (Figures 6, S35 and S37): (1) pseudorotational angles (P) and pucker amplitude (ν_{max}) that indicate ribose sugars adopting a C3′-endo conformation in the North region; (2) torsion angles ($\alpha, \beta, \gamma, \delta, \varepsilon, \zeta, \chi$) that fall in the range of a typical A-form duplex; (3) C2′-OH dihedral angle (κ) in the expected range, which provides an indication of the directionality changes arising from the presence of the aromatic ring;[38] and phosphate-phosphate distances, in the range of

Table 5. Pseudorotational Angle (P), Pucker Amplitude (ν), and Torsion Angles, Measured for Models Generated Using M06-2X/6G*[a]

entry	# Na atoms	P (deg)	ν_max	χ	α	β	γ	d	ε	ζ	κ
52	0	7.5 ± 18.6	38.5 ± 10.6	−163.3 ± 17.2	−54.9 ± 38.6	162.1 ± 31.1	55.6 ± 19.1	86.1 ± 13.4	−146.5 ± 27.3	−75.5 ± 33.9	25.7 ± 148.4
53	6	10.3 ± 24.1	41.3 ± 10.9	−160.7 ± 11.9	−117.8 ± 119.9	153.8 ± 79.9	50.9 ± 21.5	81.1 ± 19.9	−149.7 ± 60.9	−74.9 ± 73.2	−75.5 ± 137.9
54	10	6.8 ± 8.4	44.7 ± 16.7	−182.8 ± 48.4	−97.5 ± 61.9	149.2 ± 67.2	60.3 ± 7.4	78.7 ± 12.9	−107.9 ± 94.5	−107.3 ± 78.3	−30.1 ± 84.9
55	16	1.1 ± 19.3	43.6 ± 6.9	−174.9 ± 49.9	−89.4 ± 61.4	133.9 ± 63.5	64.2 ± 22.3	79.9 ± 19.7	−119.3 ± 83.5	−89.1 ± 86.1	−45.4 ± 133.9

[a]Standard deviation values larger than 25% of the average value, shown, were considered as angles leading to a larger structural impact.

https://doi.org/10.1021/acsomega.2c04784
ACS Omega 2022, 7, 37782−37796

established values for an A-form duplex, between 5.4 and 7.9 Å.[39] At the onset of this investigation, we expected angle measurements that would be in the range of the reported C2′-O-thiophenyl analog, with differences on the δ and κ angles that indicated a more compact A-form duplex.[20] However, analyses of the duplex containing four benzothiophene rings on each strand led to a pseudorotational angle (P), that while still in the North region, displayed angles that fall between the C3′-endo and C2′-exo pucker conformations (Figures 6B, S35 and S36). Importantly, this conformational change was mainly observed for internal positions, containing the BT modifications, suggesting that the presence of this aromatic ring induces a conformational change on the ribose, and places the BT ring toward the exo face of the ribose ring. Analyses of the torsion angles, along the phosphate backbone and nucleobase, displayed significant differences for angles α, γ, ζ, and κ. Variations in κ, with large standard deviations, are consistent with the existence of ribose conformational changes, toward the C2′-exo, which places the benzothiophene ring on varying positions throughout the strands. The larger deviations in the other three angles (α, γ, ζ, Table 5, entry S2) are consistent with disordered arrangements within the duplex and that may be synergistic, where the rotation around the C2′-*O*-position imposes a structural change along the ribose and impacts the α- and ζ-dihedral angles, located at the phosphate connection.

We then turned our attention to the impact of increased [Na^+] and modeled the modified duplex in the presence of varying amounts of sodium. To this end, 6, 10, or 16 sodium atoms were added to random positions around the phosphate backbone (entries 52−55). The models displayed sodium cations that were closely associated with the corresponding oxygen anion on the phosphate backbone, with reasonable/expected[40] distances of approximately 2−2.3 Å; there was only one exception (in the model containing 16 Na atoms) where one sodium cation was closer to an −OH group from the ribose. Interestingly, the incorporation of the monocation led to more pronounced angle discrepancies within the duplex, as significant deviations were observed upon measurement of several dihedral angles (α, β, ε, ζ, χ). Furthermore, the measured P−P distances are within the scope of an A-form duplex (Figure S35). These observations are consistent with the significant structural changes observed experimentally, via CD, as a function of [Na], and provide a valuable representation that aids in rationalizing the obtained results.

DISCUSSION

This work was motivated by the concept that high thermal stabilization could be achieved via the introduction of aromatic rings at the C2′-position, specifically, by a previous observation from our group, where the incorporation of eight thiophene rings on dodecamers of RNA (four on each strand) led to duplex stabilization, without impacting the A-form nature of the RNA.[7] We decided to incorporate a slightly larger group and prepared complementary strands of RNA and DNA, containing benzothiophene-methyl groups at the C2′-*O*-position. The presence of four benzothiophene rings on each strand led to stabilization of the duplex in a salt-dependent manner, specifically, sodium and magnesium. Contrary to previous observations, CD spectra for these constructs displayed two bands with positive ellipticity at 235 and 265 nm, suggesting a distinct structural motif. To explain this observation, we considered the formation of a Z_R-form duplex,[41] or a duplex similar to a "zipper" array,[42] where close interactions between the BT rings would be present, where the latter may be a more plausible option, due to the high molar ellipticity coinciding with the observed band at the λ_{max} of the benzothiophene ring (approximately 230−235 nm, Figure 1). Importantly, the stability of the duplexes was dependent on salt concentration, temperature, and position/number of benzothiophene rings. Increasing the mono-, or divalent, cation content has been established to increase duplex stability;[43,44] however, there were significant differences when the BT rings were present.

- As in our previous report, with the thiophene analogues, placing the BT aromatic rings on one strand led to significant duplex destabilization. However, contrary to that report, functionalizing both strands within the duplex did not lead to thermal stabilization; in addition, the appearance of a band with positive ellipticity at 235 nm was present, which suggested cooperativity/interactions between the BT rings, where this type of behavior has been reported on RNA duplexes containing 10 pyrene units (five on each strand) to form a zipper array.[45]
- Aiming to increase the thermal stability of the BT-modified duplex, the salt concentration was increased. This led to an unexpected observation, where the thermal stability was dramatically increased and with the appearance of more than one thermal transition (Figure 2), a phenomenon that was more marked when changing the salt to sodium perchlorate (Tables 2 and 3), with a concomitant supramolecular rearrangement, upon heating. To rationalize this, we considered that aqueous solutions in high [$NaClO_4$] can lead to high viscosity at higher temperatures and achieve a quasi-crystalline short-range local order,[46] thus potentially leading to different structural motifs. To validate these assumptions, thermal denaturation transitions were carried out in solutions containing glycerol; however, the obtained T_m values and curves displayed similar features and values as those in the absence of glycerol (Figure S38). Furthermore, the same curve was reproduced on DNA samples in high [NaCl] (Figure 4), thus ruling out an induced viscosity impact. Altogether, the differences may be due to an ionic effect on the benzothiophene rings. This was supported via modeling, where increasing the number of sodium atoms led to structural changes on the duplex, overall (Table 5). The fact that the T_m values at 235 and 260 nm are the same indicates a high degree of cooperativity among the BT-units and nucleobases.[47]

  In regards to the observed transition, and given the gathered information, we are proposing a model where (1) the benzothiophene units may interact with each other, stronger in higher monocation content, and the nucleobase interactions (base pair H-bonding or $\pi-\pi$ stacking) are disrupted; (2) upon heating, the abnormal base pair H-bonding interactions show signs that disruption/breakage starts to occur; (3) the hydrophobic benzothiophene rings aid to maintain the structure in place and allow for another internal H-bond rearrangement (much like a duplex transition, A- to Z-form[48]) into a more thermodynamically stable structure, resulting in optimal nucleobase interactions; and (4) increased temperatures lead to denaturation of the duplex. Regarding proposed step 3, temperature- and salt-dependent transitions are known, and an A- to Z-form duplex transition was recorded in a temperature depend-

https://doi.org/10.1021/acsomega.2c04784
ACS Omega 2022, 7, 37782−37796

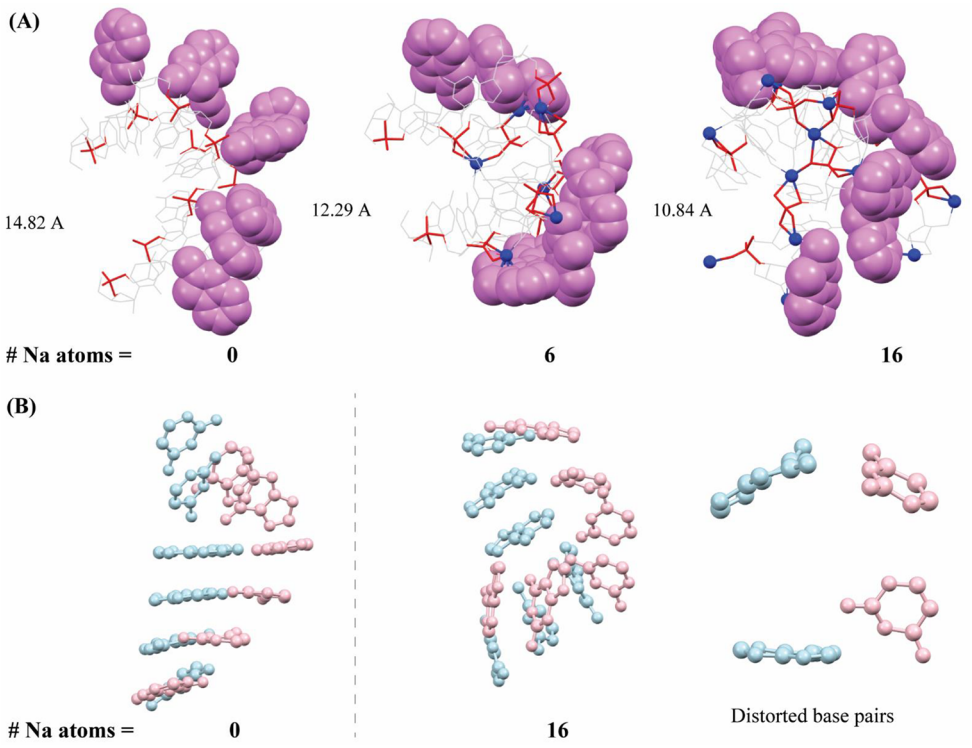

Figure 7. Side-by-side comparison of RNA duplex **4**:**7** modeled with the functional theory M06-2X/6G*, as a function of sodium content. (A) Hydrogen atoms were omitted for clarity, phosphate linkages (PO_4^-) are represented with red sticks, sodium atoms are in colored blue spheres, and benzothiophene rings are highlighted in violet as space-filling, and all other atoms are colored in light gray; (B) only nucleobases are shown for models w/wo sodium, and two examples of the distorted base pairing in the presence of Na.

ent manner, where the Z-form was generated at 45 °C using high monovalent cation concentrations ($NaClO_4$, up to 6 M).[23] Transitions that are similar to those reported here are not common; however, something similar, albeit less intense, was reported with DNA containing pyrene units at the nucleobase.[49] All studies describing such arrays do not exhibit the stabilization observed in this work, presumably because the salt concentration was increased substantially herein. It is also possible that the nature of the ends play a role, when comparing DNA and RNA, where a B-form to A-form transition has been reported by addition of a 3′-terminal ribose.[50]

- The observed binding to Zα is, in part, supported by this model, where the protein formed a complex with the modified duplexes in a [Na^+] manner. Attempts to induce a Z-form duplex on the canonical RNA were unsuccessful in our hands, and only features of an A-form structure were obtained, presumably due to the sequence context.[51,52] In this regard, we are proposing that the protein may bind to specific arrays that are formed under a specific set of conditions. The exact nature of this affinity is an area under current exploration in our laboratory.
- The nature of the loss of signal, as a function of time (Figure 3), is intriguing and still under study in our group. It is possible that a yet to be determined supramolecular arrangement, or the formation of aggregates, is giving rise to this behavior. The fact that the signal decays, without showing evidence for denaturation, suggests that the duplex structure is still present.

To rationalize the structural changes, BT-modified RNA duplex was modeled while varying the amount of sodium atoms. Measuring the pseudorotational angles on the ribose displayed changes that indicate that modified positions may adopt a C2′-exo conformation (Figure 6B), which specifically positions the BT-modification toward the exo-face.[53] It is worth noting that this is not a commonly observed conformation, while having potentially interesting properties in designing probes.[54] As depicted in Figure 7A, the proximity among benzothiophene rings becomes more prominent as more sodium atoms are incorporated. Furthermore, the distance between the phosphorus atoms located at the 5′- and 3′-ends of the same strand decreases as the [Na] increases, which suggests that the duplex is more compact and more hydrophobic. In support of this, an increase in weak interactions such as $\pi-\pi$ stacking and potential chalcogen bonding,[55] as well as between the benzothiophene rings and sodium, was detected (Figure S39). In addition, the model shows that increased salt content leads to distorted base pair interactions (Figure 7B). This is in agreement with the proposed model, where a rearrangement to a more thermally stable duplex may be occurring from the formation of stable base pairs with increased heat, before continuing on to complete denaturation.

Overall, the measured angles and recorded discrepancies, on the model, can be related to the experimental observations as structural changes lead to decreased thermal stability and disrupted nucleobase interactions. However, more experiments are needed, such as NMR, to make definite conclusions about the changes imposed by the benzothiophenyl modification. This is ongoing work.

CONCLUSION

The peculiar behavior of an RNA/DNA benzothiophene-induced array is reported herein. Its thermal stability was

https://doi.org/10.1021/acsomega.2c04784
ACS Omega 2022, 7, 37782−37796

affected in a [monovalent] manner, and the obtained structural motif displayed binding to Zα in a salt-dependent manner (not observed in the canonical analogue). While the exact nature of this affinity is a matter that is under study in our group, the data show that it is templated by the BT rings. Overall, this behavior may be useful in the generation of biomaterials or other supramolecular arrangements. Furthermore, this work provides evidence of the value of exploring the behavior of modified oligonucleotides at various salt concentrations and conditions.

■ ASSOCIATED CONTENT

Supporting Information

The Supporting Information is available free of charge at https://pubs.acs.org/doi/10.1021/acsomega.2c04784.

Experimental procedures and full characterization for modified phosphoramites **R5**. MALDI-TOF for all oligonucleotides used. Pertinent CD spectra, T_m traces, and experiments corresponding to duplex stability, Zα-binding, and viscosity. Electrophoretic analysis displaying Zα-duplex complex formation. Analyses and figures illustrating and highlighting results associated with the modeling XYZ coordinates for duplex **4:7** using all levels of theory, with varying sodium content (PDF)

■ AUTHOR INFORMATION

Corresponding Authors

Marino J. E. Resendiz − *Department of Chemistry, University of Colorado Denver, Denver, Colorado 80204, United States;* orcid.org/0000-0001-5631-2722; Email: marino.resendiz@ucdenver.edu

Haobin Wang − *Department of Chemistry, University of Colorado Denver, Denver, Colorado 80204, United States;* orcid.org/0000-0002-3532-7770; Email: haobin.wang@ucdenver.edu

Authors

Cheyenne N. Phillips − *Department of Chemistry, University of Colorado Denver, Denver, Colorado 80204, United States*

Madeline Choi − *Department of Chemistry, University of Colorado Denver, Denver, Colorado 80204, United States*

Kim Ngan Huynh − *Department of Chemistry, University of Colorado Denver, Denver, Colorado 80204, United States*

Complete contact information is available at: https://pubs.acs.org/10.1021/acsomega.2c04784

Notes

The authors declare no competing financial interest.

■ ACKNOWLEDGMENTS

C.P. would like to acknowledge UROP awards (RaCAS, CU Denver) as well as Eureca grants (CU Denver) for support. Characterization of oligonucleotides was carried out at (1) the Analytical Resources Core-Bioanalysis & Omics Facility at Colorado State University with help from Ms. Kitty Brown; or (2) the University of Colorado's Bruker Center for Excellence (Department of Pharmaceutical Sciences, Skaggs School of Pharmacy and Pharmaceutical Sciences, The University of Colorado Anschutz Medical Campus), partially funded by the L.S. Skaggs Professorship and NIH Grant R35GM128690, under the guidance of Mr. Justin Jens (laboratory of Prof. Vanessa V. Phelan); or at the Proteomics and Metabolomics Facility at Colorado State University (resource ID: SCR_021758). M.J.E.R. acknowledges support from NIGMS, via 1R15GM132816. The work was also supported by a Teacher-Scholar Award (M.J.E.R.), TH-21-028, from the Henry Dreyfus Foundation. H.W. acknowledges the support from the National Science Foundation CHE-1954639. This work used the Extreme Science and Engineering Discovery Environment (XSEDE), which is supported by NSF Grant No. ACI-1548562, and resources of the National Energy Research Scientific Computing Center (NERSC), which is supported by the Office of Science of the U.S. Department of Energy under Contract No. DE-AC02-05CH11231. The following individuals had a role in developing the synthetic route of the phosphoramidites described in this work (in alphabetical order): Ms. Paula G. Lewis, Mr. Diego J. Minjares, and Mr. Lamont Sharp. The authors would like to thank Prof. Quentin Vicens, Prof. Beat Vögeli, and Mr. Parker Nichols (CU Anschutz) for a donation of the Zα-protein that was used in this work.

■ REFERENCES

(1) Glazier, D. A.; Liao, J.; Roberts, B. L.; Li, X.; Yang, K.; Stevens, C. M.; Tang, W. Chemical synthesis and biological application of modified oligonucleotides. *Bioconjugate Chem.* **2020**, *31*, 1213−1233.

(2) Hu, B.; Zhong, L.; Weng, Y.; Peng, L.; Huang, Y.; Zhao, Y.; Liang, X.-J. Therapeutic siRNA: state of the art. *Sig Transduct Target Ther.* **2020**, *5*, 101.

(3) Dunn, M. R.; Jimenez, R. M.; Chaput, J. C. Analysis of aptamer discovery and technology. *Nat. Rev.* **2017**, *1*, 0076.

(4) Anosova, I.; Kowal, E. A.; Dunn, M. R.; Chaput, J. C.; Van Horn, W. D.; Egli, M. The structural diversity of artificial genetic polymers. *Nucleic Acids Res.* **2016**, *44*, 1007−1021.

(5) Egli, M.; Manoharan, M. Ree-engineering RNA molecules into therapeutic agents. *Acc. Chem. Res.* **2019**, *52*, 1036−1047.

(6) Hrdlicka, P. J.; Karmakar, S. 25 years and still going strong: 2′-O-(pyren-1-yl)methyl ribonucleotides − versatile building blocks for applications in molecular biology, diagnostics, and material science. *Org. Biomol. Chem.* **2017**, *15*, 9760−9774.

(7) Nguyen, J. C.; Dzowo, Y. K.; Wolfbrandt, C.; Townsend, J.; Kukatin, S.; Wang, H.; Resendiz, M. J. E. Synthesis, Thermal Stability, Biophysical Properties, and Molecular Modeling of Oligonucleotides of RNA Containing 2′-O-2-thiophenylmethyl Groups. *J. Org. Chem.* **2016**, *81* (19), 8947−8958.

(8) Gupta, P.; Langkjaer, N.; Wengel, J. Synthesis and biophysical studies of coronene functionalized 2′-amino-LNA: A novel class of fluorescent nucleic acids. *Bioconjugate Chem.* **2010**, *21*, 513−520.

(9) Anderson, B. A.; Onley, J. J.; Hrdlicka, P. J. Recognition of double-stranded DNA using energetically activated duplexes modified with N2′-pyrene-, perylene-, or coronene-functionalized 2′-*N*-methyl-2′-amino-DNA monomers. *J. Org, Chem.* **2015**, *80*, 5395−5406.

(10) Kenski, D. M.; Butora, G.; Willingham, A. T.; Cooper, A. J.; Fu, W.; Qi, N.; Soriano, F.; Davies, I. W.; Flanagan, W. M. siRNA-optimized modifications for enhanced *in vivo* activity. *Mol. Ther. Nucleic Acids* **2012**, *1*, e5.

(11) Košutić, M.; Jud, L.; Da Veiga, C.; Frener, M.; Fauster, K.; Kreutz, C.; Ennifar, E.; Micura, R. Surprising base pairing and structural properties of 2′-trifluoromethylthio-modified ribonucleic acids. *J. Am. Chem. Soc.* **2014**, *136*, 6656−6663.

(12) Tanpure, A. A.; Balasubramanian, S. Synthesis and multiple incorporations of 2′-O-methyl-5-hydroxymethylcytidine, 5-hydroxymethylcytidine and 5-formylcytidine monomers into RNA oligonucleotides. *ChemBioChem.* **2017**, *18*, 2236−2241.

(13) Richardson, J. S.; Schneider, B.; Murray, L. W.; Kapral, G. J.; Immormino, R. M.; Headd, J. J.; Richardson, D. C.; Ham, D.; Hershkovits, E.; Williams, L. D.; Keating, K. S.; Pyle, A. M.; Micallef, D.; Westbrook, J.; Berman, H. M. RNA backbone: Consensus all-angle conformers and modular string nomenclature (an RNA ontology consortium contribution. *RNA* **2008**, *14*, 465−481.

(14) Evich, M.; Spring-Connell, A. M.; Germann, M. W. Impact of modified ribose sugars on nucleic acid conformation and function. *Heterocycl. Commun.* **2017**, *23*, 155−165.
(15) Lescrinier, E.; Froeyen, M.; Herdewijn, P. Difference in conformational diversity between nucleic acids with a six-membered 'sugar' unit and natural 'furanose' nucleic acids. *Nucleic Acids Res.* **2003**, *31*, 2975−2989.
(16) Lesnik, E. A.; Freier, S. M. What affects the effect of 2′-alkoxy modifications? 1. Stabilization effect of 2′-methoxy substitutions in uniformly modified DNA oligonucleotides. *Biochemistry* **1998**, *37*, 6991−6997.
(17) Lesnik, E. A.; Guinosso, C. J.; Kawasaki, A. M.; Sasmor, H.; Zounes, M.; Cummins, L. L.; Ecker, D. J.; Cook, P. D.; Freier, S. M. Oligodeoxynucleotides containing 2′-*O*-modified adenosine: Synthesis and effects on stability of DNA:RNA duplexes. *Biochemistry* **1993**, *32*, 7832−7838.
(18) Nagaya, Y.; Kitamura, Y.; Shibata, A.; Ikeda, M.; Akao, Y.; Kitade, Y. Introduction of 2-*O*-benzyl abasic nucleosides to the 3′-overhang regions of siRNAs greatly improves nuclease resistance. *Bioorg. Med. Chem. Lett.* **2017**, *27*, 5454−5456.
(19) Nakamura, M.; Fukunaga, Y.; Sasa, K.; Ohtoshi, Y.; Kanaori, K.; Hayashi, H.; Nakano, H.; Yamana, K. Pyrene is highly emmisive when attached to the RNA duplex but not to the DNA duplex: the structural basis of this difference. *Nucleic Acids Res.* **2005**, *33*, 5887−5895.
(20) Dzowo, Y. K.; Wolfbrandt, C.; Resendiz, M. J. E.; Wang, H. Modeling of canonical and C2′-O-thiophenylmethyl modified hexamers of RNA. Insights into the nature of structural changes and thermal stability. *New J. Chem.* **2018**, *42*, 10177.
(21) Schowe, S. W.; Langeberg, C. J.; Chapman, E. G.; Brown, K.; Resendiz, M. J. E. Identification of RNA fragments resulting from enzymatic degradation using MALDI-TOF mass spectrometry. *J. Vis. Exp.* **2022**, *182*, e63720.
(22) Nichols, P. J.; Bevers, S.; Henen, M.; Kieft, J. S.; Vicens, Q.; Vögeli, B. Recognition of non-CpG repeats in Alu and ribosomal RNAs by the Z-RNA binding domain of ADAR1 induces A-Z junctions. *Nat. Commun.* **2021**, *12*, 793.
(23) O'Hara, C.; Yang, C.-H.; Francis, A.; Newell, B.; Wang, H.; Resendiz, M. J. E. Photocycloaddition of S,S-Dioxo-benzothiophene-2-methanol, Reactivity in the Solid State and in solution: Mechanistic Studies and Diastereoselective Formation of Cyclobutyl Rings. *J. Org. Chem.* **2019**, *84*, 9714−9725.
(24) Schiel, M. A.; Domini, C. E.; Chopa, A. B.; Silbestri, G. F. Microwave-assisted syntheses of thiophene-based ionic liquids: Structural design and optimization. *Synthesis* **2018**, *50*, 4846−4854.
(25) Hall, K.; Cruz, P.; Tinoco, I., Jr.; Jovin, T. M.; van de Sande, J. H. Z-RNA' − a Left-Handed RNA Double Helix. *Nature* **1984**, *311*, 584−586.
(26) Hardin, C. C.; Zarling, D. A.; Puglisi, J. D.; Trulson, M. O.; Davis, P. W.; Tinoco, I., Jr. Stabilization of Z-RNA by Chemical Bromination and its Recognition by Anti-Z-DNA Antibodies. *Biochemistry* **1987**, *26*, 5191−5199.
(27) Balasubramaniyam, T.; Ishizuka, T.; Xiao, C.-D.; Bao, H.-L.; Xu, Y. 2′-*O*-Methyl-8-methylguanosine as a Z-Form RNA Stabilizer for Structural and Functional Study of Z-RNA. *Molecules* **2018**, *23*, 2572.
(28) Shen, F.; Luo, Z.; Liu, H.; Wang, R.; Zhang, S.; Gan, J.; Sheng, J. Structural insights into RNA duplexes with multiple 2′-5′-linkages. *Nucleic Acids Res.* **2017**, *45*, 3537−3546.
(29) Waters, J. T.; Lu, X.-J.; Galindo-Murillo, R.; Gumbart, J. C.; Kim, H. D.; Cheatham, T. E., III; Harvey, S. C. Transitions of double-stranded DNA between the A- and B-forms. *J. Phys. Chem. B* **2016**, *120*, 8449−8456.
(30) Kelly, S. M.; Jess, T. J.; Price, N. C. How to study proteins by circular dichroism. *Biochem. Biophys. Acta* **2005**, *1751*, 119−139.
(31) Barone, V.; Cossi, M.; Tomasi, J. A new definition of cavities for the computation of solvation free energies by the polarizable continuum model. *J. Chem. Phys.* **1997**, *107*, 3210−3221.
(32) Cammi, R.; Mennucci, B.; Tomasi, J. On the Calculation of Local Field Factors for Microscopic Static Hyperpolarizabilities of Molecules in Solution with the Aid of Quantum-Mechanical Methods. *J. Phys. Chem. A* **1998**, *102*, 870−875.
(33) Cammi, R.; Mennucci, B.; Tomasi, J. An Attempt To Bridge the Gap between Computation and Experiment for Nonlinear Optical Properties: Macroscopic Susceptibilities in Solution. *J. Phys. Chem. A* **2000**, *104*, 4690−4698.
(34) Gaussian 16, Revision C.01 ,Frisch, M. J.; Trucks, G. W.; Schlegel, H. B.; Scuseria, G. E.; Robb, M. A.; Cheeseman, J. R.; Scalmani, G.; Barone, V.; Petersson, G. A.; Nakatsuji, H.; Li, X.; Caricato, M.; Marenich, A. V.; Bloino, J.; Janesko, B. G.; Gomperts, R.; Mennucci, B.; Hratchian, H. P.; Ortiz, J. V.; Izmaylov, A. F.; Sonnenberg, J. L.; Williams-Young, D.; Ding, F.; Lipparini, F.; Egidi, F.; Goings, J.; Peng, B.; Petrone, A.; Henderson, T.; Ranasinghe, D.; Zakrzewski, V. G.; Gao, J.; Rega, N.; Zheng, G.; Liang, W.; Hada, M.; Ehara, M.; Toyota, K.; Fukuda, R.; Hasegawa, J.; Ishida, M.; Nakajima, T.; Honda, Y.; Kitao, O.; Nakai, H.; Vreven, T.; Throssell, K.; Montgomery, J. A., Jr.; Peralta, J. E.; Ogliaro, F.; Bearpark, M. J.; Heyd, J. J.; Brothers, E. N.; Kudin, K. N.; Staroverov, V. N.; Keith, T. A.; Kobayashi, R.; Normand, J.; Raghavachari, K.; Rendell, A. P.; Burant, J. C.; Iyengar, S. S.; Tomasi, J.; Cossi, M.; Millam, J. M.; Klene, M.; Adamo, C.; Cammi, R.; Ochterski, J. W.; Martin, R. L.; Morokuma, K.; Farkas, O.; Foresman, J. B.; Fox, D. J. Gaussian, Inc.: Wallingford, CT, 2016.
(35) Grimme, S.; Antony, J.; Ehrlich, S.; Krieg, H. A consistent and accurate ab initio parametrization of density functional dispersion correction (DFT-D) for the 94 elements H-Pu. *J. Chem. Phys.* **2010**, *132*, 154104.
(36) Zhao, Y.; Truhlar, D. G. The M06 suite of density functionals for main group thermochemistry, thermochemical kinetics, noncovalent interactions, excited states, and transition elements: two new functionals and systematic testing of four M06-class functionals and 12 other functionals. *Theor. Chem. Acc.* **2008**, *120*, 215−241.
(37) Altona, C.; Sundaralingam, M. Conformational analysis of the sugar ring in nucleosides and nucleotides. New description using the concept of pseudorotation. *J. Am. Chem. Soc.* **1972**, *94*, 8205−8212.
(38) Darré, L.; Ivani, I.; Dans, P. D.; Gómez, H.; Hospital, A.; Orozco, M. Small details matter: The 2′-hydroxyl as a conformational switch in RNA. *J. Am. Chem. Soc.* **2016**, *138*, 16355−16363.
(39) Draper, D. E. Folding of RNA tertiary structure: Linkages between backbone phosphate, ions, and water. *Biopolymers* **2013**, *99*, 1105−1113.
(40) Schneider, B.; Kabeláč, M.; Hobza, P. Geometry of phosphate group and its interactions with metal cations in crystals and *ab Initio* calculations. *J. Am. Chem. Soc.* **1996**, *118*, 12207−12217.
(41) Trulson, M. O.; Cruz, P.; Puglisi, J. D.; Tinoco, I., Jr.; Mathies, R. A. Raman spectroscopic study of left-handed Z-RNA. *Biochemistry* **1987**, *26*, 8624−8630.
(42) Nakamura, M.; Murakami, Y.; Sasa, K.; Hayashi, H.; Yamana, K. Pyrene-zipper array assembled via RNA duplex formation. *J. Am. Chem. Soc.* **2008**, *130*, 6904−6905.
(43) Urata, H. Effect of chirality of ribose on nucleic acid structure and function. *Yakugaku Sasshi* **1999**, *119*, 689−709.
(44) Serra, M. J.; Baird, J. D.; Dale, T.; Fey, B. L.; Retatagos, K.; Westhof, E. Effects of magnesium ions on the stabilization of RNA oligomers of defined structures. *RNA* **2002**, *8*, 307−323.
(45) Nakamura, M.; Fukuda, M.; Takada, T.; Yamana, K. Highly ordered pyrene π-stacks on an RNA duplex display static excimer fluorescence. *Org. Biomol. Chem.* **2012**, *10*, 9620−9626.
(46) Miller, M. L.; Doran, M. Concentrated salt solutions. II. Viscosity and density of sodium thiocyanate, sodium perchlorate and sodium iodide. *J. Phys. Chem.* **1956**, *60*, 186−189.
(47) Dietzxch, J.; Bialas, D.; Bandorf, J.; Würthner, F.; Höbartner, C. Tuning exciton coupling of merocyanine nucleoside dimers by RNA, DNA and GNA double helix conformations. *Angew. Chem., Int. Ed.* **2022**, *61*, e202116783.
(48) Kastenholz, M. A.; Schwartz, T. U.; Hunenberger, P. H. The transition between the B and Z conformation of DNA investigated by targeted molecular dynamics simulations with explicit solvation. *Biophys. J.* **2006**, *91*, 2976−2990.

https://doi.org/10.1021/acsomega.2c04784
ACS Omega 2022, 7, 37782−37796

(49) Kim, K. T.; Heo, W.; Joo, T.; Kim, B. H. Photophysical and structural investigationof a ^{Py}A-modified adenine cluster: its potential use for fluorescent DNA probes exhibiting distinct emission color changes. *Org. Biomol. Chem.* **2015**, *13*, 8470−8478.
(50) Wahl, M. C.; Sundaralingam, M. B-form to A-form conversion by a 3′-terminal ribose: crystal structure of the chimera d(CCACTAGTFr-(G). *Nucleic Acids Res.* **2000**, *28*, 4356−4363.
(51) Wang, A. H-J.; Quigley, G. J.; Kolpak, F. J.; Crawford, J. L.; van Boom, J. H.; van der Marel, G.; Rich, A. Molecular structure of a left-handed double helical DNA fragment at atomic resolution. *Nature* **1979**, *282*, 680−686.
(52) Hardin, C. C.; Zarling, D. A.; Puglisi, J. D.; Trulson, M. O.; Davis, P. W.; Tinoco, I., Jr. Stabilization of Z-RNA by chemical bromination and its recognition by anti-Z-DNA antibodies. *Biochemistry* **1987**, *26*, 5191−5199.
(53) Li, L.; Szostak, J. W. The free enerty landscape of pseudorotation in 3′-5′ and 2′-5′ linked nucleic acids. *J. Am. Chem. Soc.* **2014**, *136*, 2858−2865.
(54) White, N. A.; Sumita, M.; Marquez, V. E.; Hoogstraten, C. G. Coupling between conformational dynamics and catalytic function at the active site of the lead-dependent ribozyme. *RNA* **2018**, *24*, 1542−1554.
(55) Pascoe, D. J.; Ling, K. B.; Cockroft, S. L. The origin of chalcogen-bonding interactions. *J. Am. Chem. Soc.* **2017**, *139*, 15160−15167.

https://doi.org/10.1021/acsomega.2c04784
ACS Omega 2022, 7, 37782−37796